metals

MDPI

Article

Study on Construction Molding Technology of Long-Span Space Truss Suspended Dome Structure

Mingliang Liu [1,2], Junhai Zhao [1,*], Yongkang Jiao [3], Cun Hui [3], Chunjuan Zhou [2], Xiao Yang [2] and Yupeng Zhang [2]

[1] School of Civil Engineering, Chang'an University, Xi'an 710061, China
[2] Shaanxi Academy of Building Research Co., Ltd., Xi'an 710082, China
[3] School of Architecture and Civil Engineering, Zhongyuan University of Technology, Zhengzhou 450007, China
* Correspondence: zhaojh@chd.edu.cn

Abstract: Typically, the upper part of the roof a gymnasium building is a radial inverted triangular truss structure, and the lower part is a cable structure. They are connected by vertical braces to form a self-balancing structural system. The whole roof is supported by a complex, spatial, prestressed structure comprising tilted Y-shaped laced columns. Such structures rely on the integrity of the form and the application of prestress to achieve the best performance; it is in an extremely unstable state during construction. In order to study the mechanical behavior of the structure in this process, finite element software was used to analyze the cumulative slip of the structure and the construction process of cable tension, and the simulation values were compared to the actual monitoring values. The stress and deformation of the structure in different construction stages were investigated, and a reasonable structural unloading scheme was put forward. The study results showed that the stiffness of the long-span space truss suspended dome structure gradually increased with the structural integrity during construction, and the vertical deformation decreased from 25.4 mm to 19.26 mm with the construction process. The location and magnitude of the structure's maximum internal force and maximum stress varied greatly compared to the static analysis when considering the construction process effects. Hence, conducting a construction process analysis is necessary. The construction technology of symmetrical rotating cumulative slip proposed in this paper has the advantages of a short construction duration, safe and stable construction process, etc., providing technical references for similar engineering constructions.

Keywords: space truss suspended dome structure; radial inverted triangular truss; prestressed construction; finite element simulation; cumulative slip

check for updates

Citation: Liu, M.; Zhao, J.; Jiao, Y.; Hui, C.; Zhou, C.; Yang, X.; Zhang, Y. Study on Construction Molding Technology of Long-Span Space Truss Suspended Dome Structure. *Metals* **2023**, *13*, 22. https://doi.org/10.3390/met13010022

Academic Editor: Piotr Paczos

Received: 13 October 2022
Revised: 18 December 2022
Accepted: 21 December 2022
Published: 22 December 2022

Copyright: © 2022 by the authors. Licensee MDPI, Basel, Switzerland. This article is an open access article distributed under the terms and conditions of the Creative Commons Attribution (CC BY) license (https://creativecommons.org/licenses/by/4.0/).

1. Introduction

Recently, building usage demand has increased with the continuity of social and economic development. Many buildings with chic designs and various functions drive structural design development in the direction of long spans and complex stress forms. As a new type of structure, the space truss suspended dome has reasonable stress-bearing capacity and can take full advantage of the performance of various materials; hence it is widely used in the construction of large public venues [1–5]. However, the number of large-scale steel bars is high, the structural stresses formed during installation are complex and changeable, the construction site is often very limited, and the construction environment factors are complicated [6]. Prior to completing the construction of the entire structure, some unit members may undergo strains and displacements during the construction process due to the difference in construction sequence, resulting in larger changes in the overall structure deflection [7,8], which makes the actual stress and strain of the members greatly different from the design values. As a result, there is great potential for a safety hazard

during construction and subsequent use. Hence, high requirements must be put forward for construction technology.

In recent years, research on space truss suspended dome structures has been deepened, and its construction technology has been continuously developed. Liu et al. [9] conducted a comparative study on the structural performance of the suspen-dome structures with different cable forms. Yan et al. [10] studied the influence of the law of random prestressed loss on structural bearing capacity through probability and statistics theory. Shen et al. [11] proposed a construction method for sectional slip in a longitudinally supported reticulated shell structure. This method is mainly used to construct closed projects such as coal sheds. Feng et al. [12] introduced a construction process of unequal high slip and analyzed the structure state during the slip process and the possible adverse effects on the slip, guaranteeing the safety and reliability of the slip construction scheme. Through theoretical analysis of the slip process, Zhou et al. [13] established a simplified model of the slip unit displacement and analyzed the main parameters leading to the asynchronization of slip units, which provides a reference for the design of the synchronous control system. Considering the size effect and friction characteristics of sliding supports in long-span structure construction, Can et al. [14] studied the support's mechanical properties and performed statistical analysis on the results, providing a reference for the design of sliding supports. Liu et al. [15,16] studied the prestress deviation caused by sliding friction and temperature in the prestress construction process, verified it experimentally and numerically, developed and verified a simplified calculation formula, and proposed several improvement measures. Fan et al. [17] studied how the friction between cables and brace joints resulted in cable force loss and proposed a construction technology combining the iteration procedure for quantifying friction force and the tension compensation method. Li et al. [18] simulated the construction error of a chord-supported structure with a stochastic imperfection model and provided some conclusions of universal significance. Du et al. [19] proposed an improved rigid cable method to deal with the prestress loss of chord-supported structures after pre-tensioning by the rigid cable method. Liu et al. [20] simulated and analyzed the whole construction process of the prestressed cable through finite element software and discussed the influence of coupling on the construction process of chord-supported structures by establishing two simulation models, i.e., coupling and uncoupling models. Liu et al. [21] proposed a form-finding algorithm with double control of arch–cable force value for ring cable tension construction technology. Zhou et al. [22] proposed a form analysis method for suspension dome structure considering the influence of the pre-tension process and verified the method with an example. Liu et al. [23], to solve the shortage of traditional construction simulation methods for suspended dome structures, put forward the cable tension pre-slack method. Teng et al. [24] designed a long-term monitoring system for Shenzhen Bay Stadium to investigate temperature and displacement changes simultaneously. This monitoring system will be widely used in the future. Thanks to the development of engineering mechanics, the theoretical calculation results are increasingly close to the actual situation [25,26]. At the same time, the influence of temperature effect is considered by referring to the simulation process of similar projects [27,28].

In order to clarify the development law of internal force and displacement of components in the construction process of the space truss suspended dome structure and reduce the adverse impact of the construction process on the structural performance, this paper applies numerical simulation techniques to model the construction process of suspended dome structures in large gymnasiums by using a finite element approach and successively establishing the construction conditions of three stages. The construction process is simulated and analyzed, and the loads are applied strictly in accordance with the selected case study's original construction sequence and method. The calculated results are used to guide the monitoring program and compare it with the field monitoring results, which can ensure the safety of the construction process and provide data support for the design and construction of similar structures in the future.

2. Project Overview

In this study, the selected gymnasium was built in Xi'an City, China and has a south–north length of 229 m, east–west width of 126 m, and a height of 37.7 m. The structure can be divided into two major parts: the main gymnasium of the center and the auxiliary gymnasium on both the north and the south sides. The overall effect of the building is shown in Figure 1. The upper dome roof in the main gymnasium is a long-span space truss suspended dome structure consisting of steel and cable parts. The steel-structured roof consists of 20 space-inverted triangular trusses. By strengthening the secondary plane truss and the ring truss, the roof is entirely connected, with each inverted triangular truss being about 48 m long. The cable structure is composed of an annular cable, a radial cable, and a brace. The overall roof is supported by 22 Y-shaped laced columns with a span of 110 m, and the lower structure is a reinforced concrete frame. The structure that forms the auxiliary gymnasium is a plane truss, with each truss supported by two frame columns. The inner truss of the auxiliary gymnasium is connected to the main gymnasium, and the outermost part is a cantilever structure. Rectangular steel pipes are used for the inner ring truss of the roof center section, and circular steel pipes are used for the inverted triangular truss, outer ring truss, and laced columns, with diameters ranging from 102 mm to 600 mm. The frame column section of the auxiliary gymnasium is ø800 mm × 20 mm, and the steel structure material of both the main and auxiliary gymnasiums is Q345B. The lower layer of the structure is composed of annular and radial cables. The cables are made with high vanadium content and have diameters ranging from 48 mm to 100 mm. Figure 2 shows the three-dimensional steel structure drawing of the main gymnasium.



Figure 1. Overall effect drawing of the building.

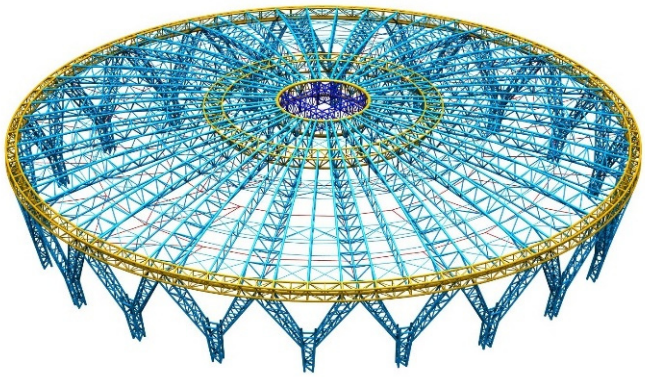


Figure 2. The three-dimensional steel structure drawing of the main gymnasium.

The structural system is based on the suspen-dome structure, and has been partially optimized; the upper structure is adjusted to the inverted triangular truss; the overall stiffness of the structure is significantly increased; the shape is beautiful and efficient; and in order to achieve the optimal structural performance, the construction process needs to accurately control the construction error.

3. Construction Scheme

The overall construction process of the steel structure in the gymnasium can be divided into the following four steps: the installation of the truss and laced columns of the main gymnasium, the installation of the central reticulated shell of the main gymnasium, the installation of the steel structure in the auxiliary gymnasium, and the installation and tensioning of the cable structure in the main gymnasium. The steel structure construction sequence is shown in Figure 3.

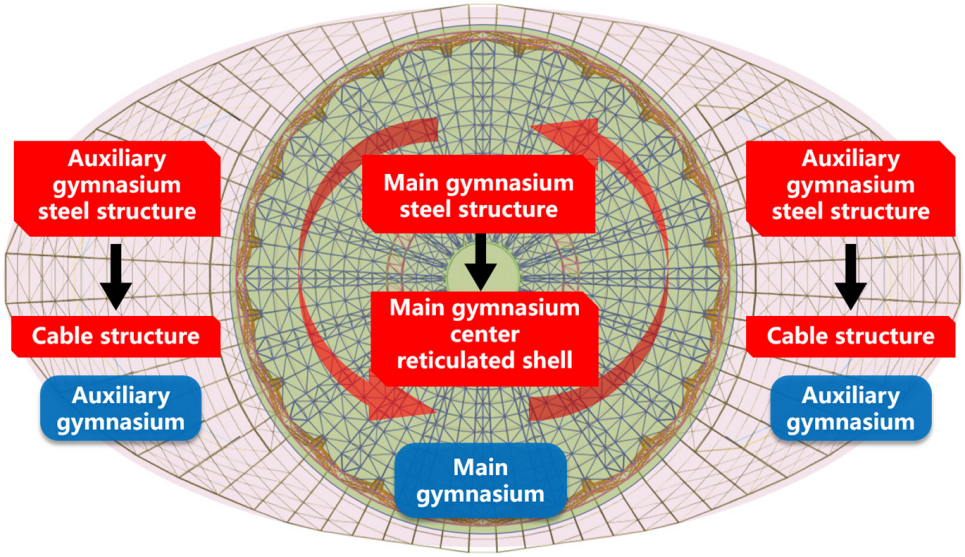


Figure 3. Illustration of the steel structure construction sequence.

3.1. Steel Structure Slip Construction in the Main Gymnasium

3.1.1. Scheme Selection

Since the space truss suspended dome structure system selected in this study has a long span, many structural units, and a large self-weight, adopting high-altitude hoisting construction results in a large workload and difficulty in ensuring high installation accuracy, which ultimately impacts the construction quality and duration. Combined with the previous construction methods of such projects, the symmetrical rotating cumulative slip construction method of "outer ring active and inner ring follow" is adopted for the main gymnasium in this project to reduce the workload of high-altitude installation, ensure the construction quality, and improve the safety of construction workers.

3.1.2. Slip Unit Division

According to the construction site conditions and the steel structure characteristics of the main gymnasium, the roof truss of the main gymnasium was divided into units, and each truss was taken as a slip element. The assembly platform (The red box in Figure 4) was set between the Z-8 axis and the Z-14 axis and between the Z-33 axis and the Z-44 axis to assemble the roof structure. The angle between the main trusses of the roof was set to 18 degrees. Taking each main truss roof as a slip unit, the entire roof was divided into 9 symmetrical units, which slipped into place 8 times, and the 9th unit was assembled in situ. The division of roof slip units and the tire frame layout is shown in Figure 4.

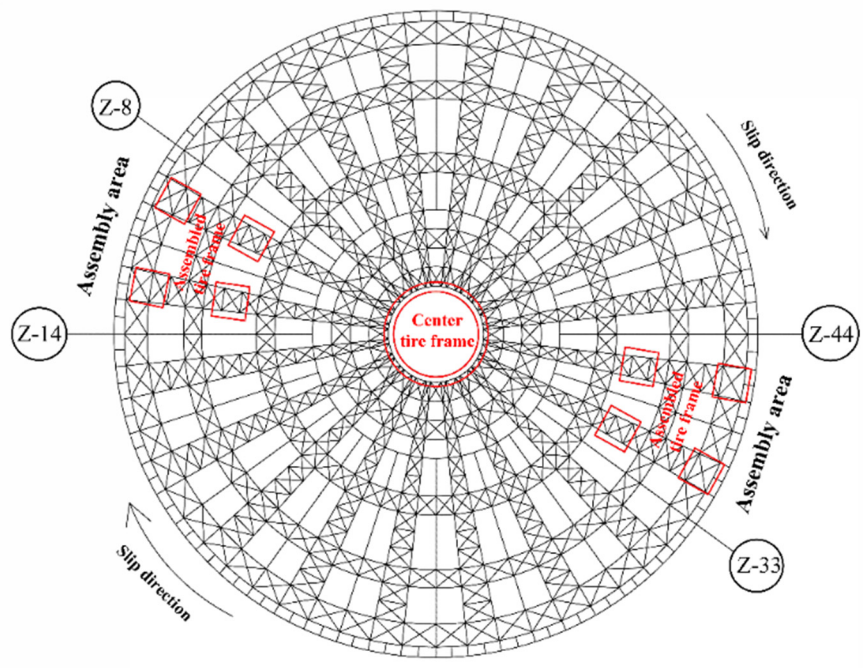
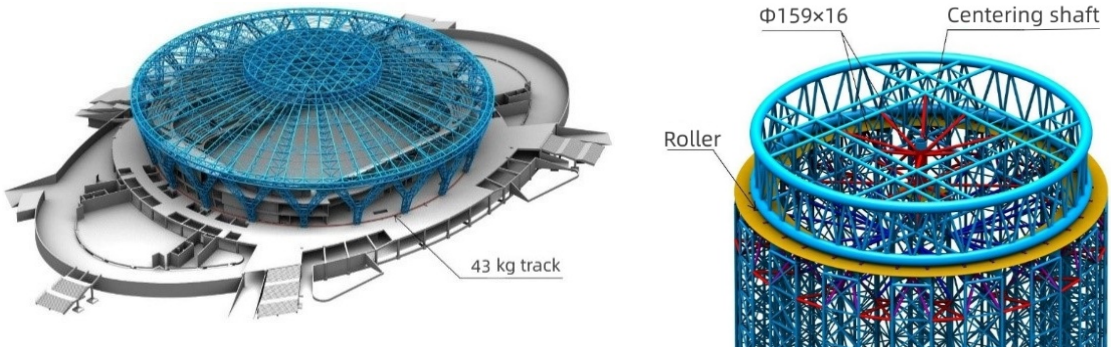


Figure 4. Layout of the Slip site.

3.1.3. Slip System Principle

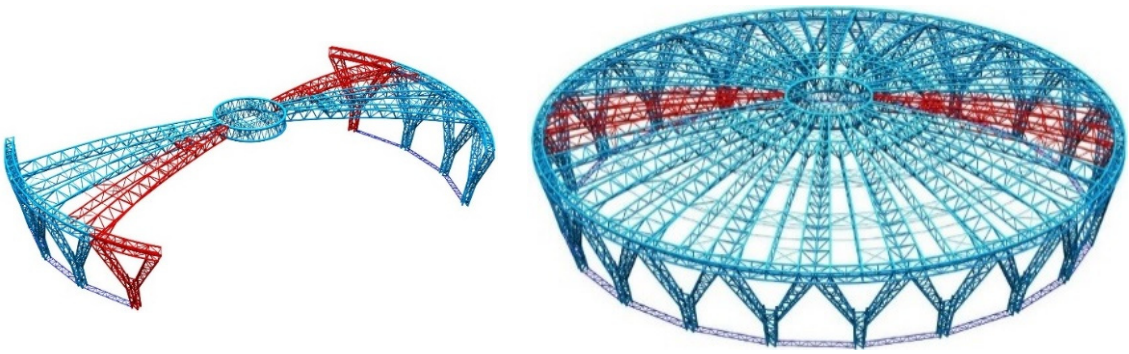
According to the project characteristics, only the outer ring slip track (a standard rail specification of 43 kg/m) was set at the foot of the laced column; a pusher was configured between every other column at each interval; and reinforcement bars were set between the column feet to enhance the integrity. No track was set on the tire frame below the inner truss ring. The inner ring truss slipped on the top of the tire frame, and a slip beam was set on the top of the temporary tire frame. Furthermore, a 70-mm-thick steel plate was placed on the upper part of the slip beam as the slip track. A roller was set above the sliding track to reduce the friction between the member of steel. The slip system is shown in Figure 5.



(**a**) (**b**)

Figure 5. Schematic diagram of the slip system. (**a**) Outer ring slip track arrangement, (**b**) central ring-supported tire frame.

Once the first slip unit was assembled, the hydraulic tractor and other slippage equipment were installed, and a tractor was installed between every other column. After the installation, the hydraulic system was adjusted, and the first assembled slip unit was slipped forward 18 degrees along the arc to stop slippage. Thereafter, the second slip unit was assembled on the assembly tire frame, and the above steps were repeated until all the slip units were in place. Finally, units 8 and 9 were assembled in situ. The structural slip process is shown in Figure 6.



(**a**) (**b**)

Figure 6. Schematic diagram of structural slip process. (**a**) The first slip unit, (**b**) the assembled main gymnasium.

3.1.4. Unloading of Steel Structure in the Main Gymnasium

When all structural units slipped to the specified position, the tractor, slipper ear plate, and temporary reinforcement rod were removed, and the unloading operation was then performed. Four jacks were set at the foot of each laced column, a steel leg was set on the side of each slipper, and the steel leg was supported by the jack to lift the roof structure. After that, the lower slip track was removed, the pin structure was installed, and the roof structure load was transferred to the pin to complete the unloading construction. The schematic diagram of steel structure unloading is shown in Figure 7.

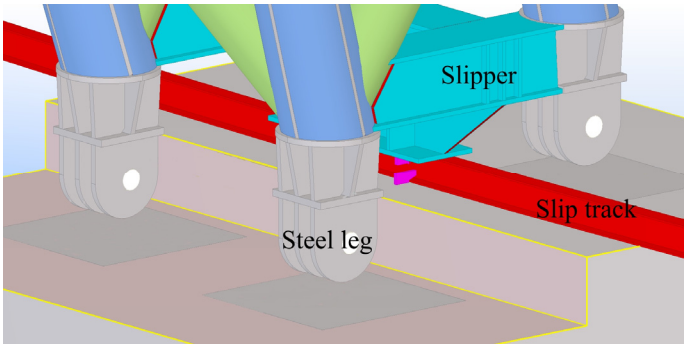


Figure 7. Unloading of steel structure in the main gymnasium.

3.2. Installation of Steel Structure in the Auxiliary Gymnasium

Upon installing the steel structure in the main gymnasium, the steel structure in the auxiliary gymnasium was installed, as shown in Figure 8. The south and north auxiliary gymnasiums were constructed simultaneously, with the installation sequence proceeding from the middle to both sides. In the auxiliary gymnasium construction, two 100-t truck cranes were used to lift steel columns and trusses, and two 25-t truck cranes were used for the backhaul of matching materials and filling in the middle. The installation sequence of the steel structure in the auxiliary gymnasium was as follows: columns close to the inner side of the main gymnasium → the lateral oblique steel columns → the middle section truss → the most lateral cantilever section truss → the connecting truss between the main and auxiliary gymnasiums.

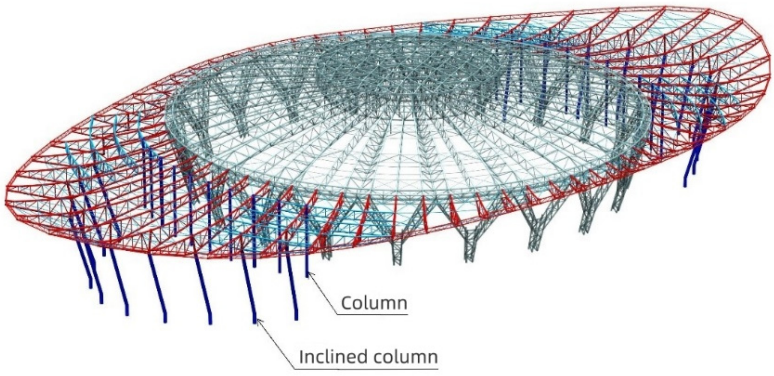


Figure 8. Schematic diagram of the steel structure in the auxiliary gymnasium.

3.3. Cable Structure Installation

Once the steel truss and the central reticulated shell in the main gymnasium were installed, the annular cables were placed, and the radial cables were assembled and tensioned. The annular cable was not tensioned. However, the radial cable was pre-tensioned from inside to outside, with a tension force of 10% of the designed tension force.

Thereafter, it was tensioned from outside to inside with 70% of the designed tension force. In this case, the steel structure roof of the main gymnasium was unloaded. After that, it was tensioned from the inside out to 100% of the design force. Finally, the stable oblique cable was installed and tensioned. The schematic diagrams for cable structure and tension sequence are shown in Figures 9 and 10.

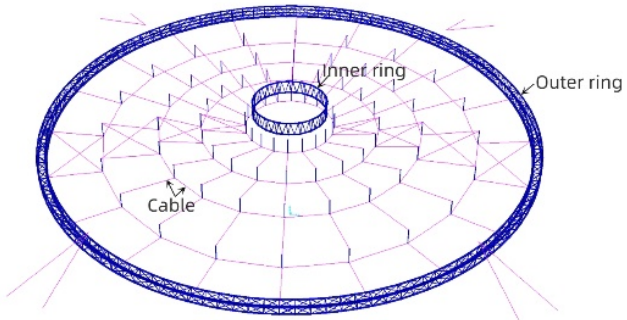


Figure 9. Schematic diagram of the cable structure.

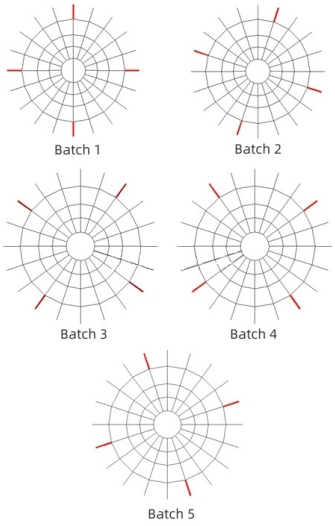


Figure 10. Schematic diagram for the tension sequence of cable structure.

4. Construction Process Simulation

Due to the construction particularity of long-span steel structures, taking the whole structure in its final state as the study object, this method is not sufficiently comprehensive for designing the structure, as it may produce unexpected displacement and deformation during the construction process. In this paper, the finite element calculation software Midas Gen was used to carry out the construction simulation of prestressed steel structures to ensure the safety of the construction process and subsequent use of the structure.

4.1. Analysis of Slip Construction Process

According to the construction scheme, the whole slip process of the structure was divided into eight stages, and the corresponding eight structural groups were defined according to the eight construction stages. In order to make the simulation calculation consistent with the actual construction process, the model was established, and then the loads were applied according to the following requirements:

1. Structural self-weight was mainly considered in construction simulation. Because self-weight is disadvantageous to structures subjected to dynamic load, the subitem coefficient for the load was taken as 1.4, and the load subitem coefficient was taken as 1.0 when checking structural displacement.
2. The laced columns and trusses were simulated using beam units, and the outer ring track slippers' position was considered hinged.
3. The slipper was checked using the finite element software ANSYS, with the unit type selected as Solid185.
4. The inner ring-supported tire frame had good overall performance, and the vertical deformation during the slip process was small. In order to simplify the calculation, the inner ring-supported tire frame was ignored, and the central ring truss was added with restricted Z-direction translation and X and Y axial rotation constraints.

4.2. Analysis of Cable Structure Tension Construction Process

In order to ensure that the model analysis results were consistent with the actual project as much as possible, the modeling calculation parameters were set as follows:

1. By considering the node weight in the reticulated shell, the value of the self-weight coefficient was enlarged to 1.05.
2. The cable structure was defined as the tension unit; the brace was defined as the beam element; the beam end constraint was released; and the prestress was applied to the structure by changing the temperature.

5. Analysis of Construction Process Results

5.1. Slip Construction Process

5.1.1. Stress Analysis

The representative construction stages of the 1st, 3rd, 5th, 6th, 7th, and 8th in the software analysis results were selected for analysis. Table 1 shows the maximum stress values of structural bars in the construction process, and Figure 11 shows the stress cloud diagram of each construction stage. It can be seen from the changes of the structure stress cloud diagram that with the gradual progress of the construction process, the structural integrity was constantly improved; the internal forces of the structural bars were also increasing; and the truss structure displacement gradually tended to stabilize. The maximum tensile stress in the structure was located at the vertical belly bar of the outer ring truss in stages 1 and 3. In stages 5 and 6, it appeared at the belly rod of the central ring truss, whereas in stage 7, it appeared at the top chord of the central ring truss, and in stage 8, it appeared at the vertical belly bar of the structure's outer ring truss. The maximum compressive stress on the structure was located at the connection between the central ring truss and the lower chord of the inverted triangular truss in the construction simulation process.

Table 1. Maximum stress values during construction from modeling.

Construction Stage	Maximum Tensile Stress of the Bar (MPa)	Maximum Compressive Stress of the Bar (MPa)
1	59.88	−117.37
3	55.96	−132.74
5	76.56	−136.85
6	82.16	−135.20
7	64.45	−128.99
8	34.15	−104.10

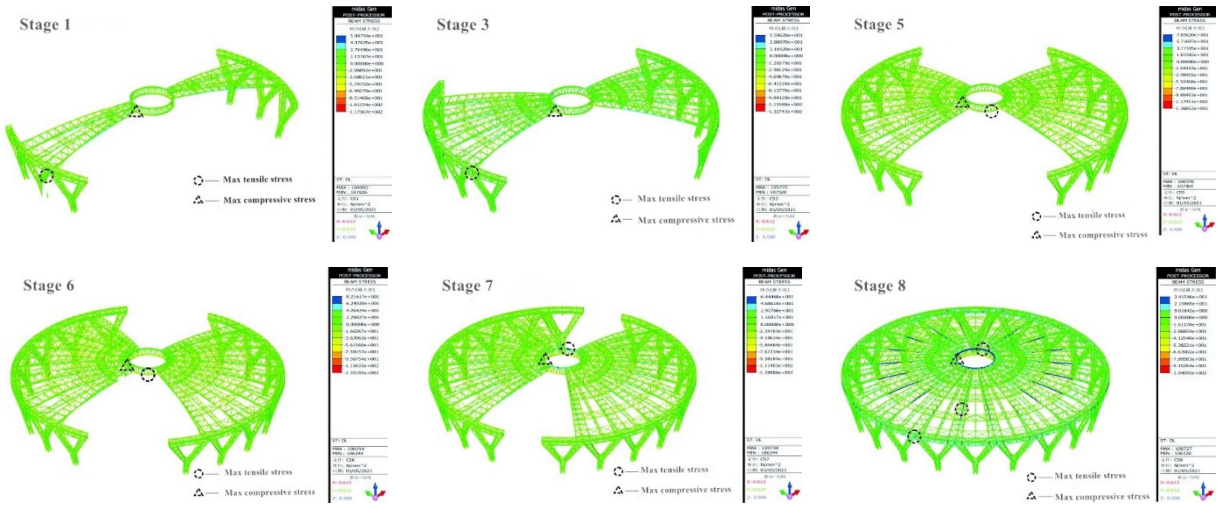


Figure 11. Cloud diagram for stress during construction.

It can be seen from Table 1 that the maximum tensile stress on the structure appeared in stage 6, and the maximum compressive stress appeared in stage 5. The stress ratio of the bars was less than 0.85, which meets the construction requirements. According to the simulation results, the stress on the vertical belly bar of the outer ring truss, that on the belly bar of the central ring truss, and that on the upper chord were concentrated. This issue should be further investigated during construction monitoring.

5.1.2. Displacement Analysis

Based on the software analysis results, the maximum structural displacement changes and displacement cloud diagrams of the 1st, 3rd, 5th, 6th, 7th, and 8th construction stages are shown in Figures 12 and 13. It can be seen that at the end of stage 1, the maximum structural displacement was located at the lower chord of the mid-span truss, then it continued to increase in the assembling process of stages 2, 3, and 4, until reaching maximum displacement in construction stage 4, during which it increased from 23.89 mm to 25.40 mm, which are all located at the lower chord of the middle truss of the structure. The deformation value was less than L/500 = 97.6 mm, which meets the construction requirements [29]. Compared with similar projects [30], the deformation of this structure was smaller, and the reason is that the main truss stiffness was larger.

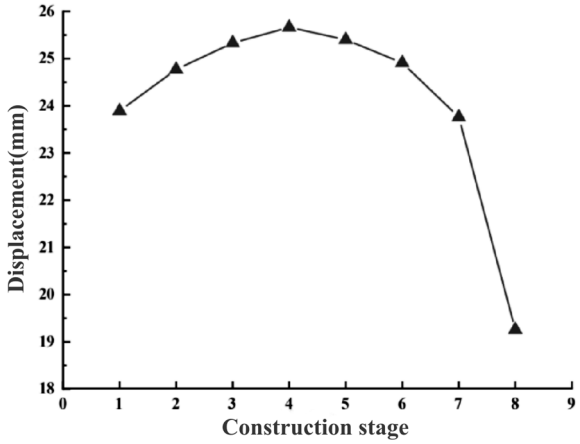


Figure 12. The maximum displacement changes in the structure.

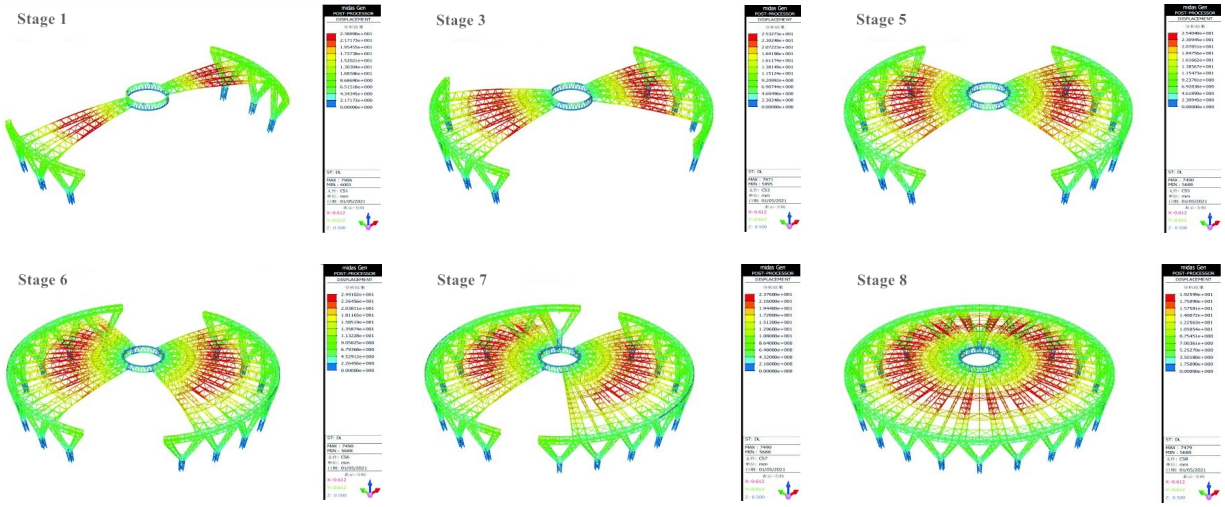


Figure 13. Cloud diagrams for displacement during construction.

According to the above analysis, due to the installation sequence, the internal force distribution of similar members was no longer uniform when they entered the operating state after the completion of structure installation. However, the structure's maximum vertical displacement was located at the lower chord of the middle truss. Therefore, close attention should be paid to the internal force and displacement changes of members in this area during construction.

It can be seen from Figures 14 and 15 that during the installation process of units 1 to 9, the vertical displacement of the control node in the span of each sliding unit increased gradually with the construction progress, and the internal force of members also increased gradually with the construction progress. This is very similar to the loading process of similar projects [31], which indicates that the installation of the following structure will increase the overall internal force and displacement of the structure. The existing structure's displacement and the existing members' internal force will accumulate continuously during the construction and installation. However, the increasing amplitude gradually decreases and finally becomes stable, indicating that the stiffness of the space truss suspended dome structure increases with the structural integrity during construction.

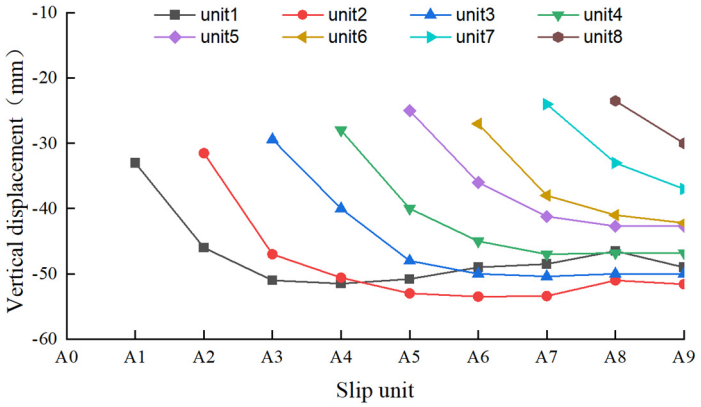


Figure 14. Displacement variation diagram of a control node in the midspan of each unit.

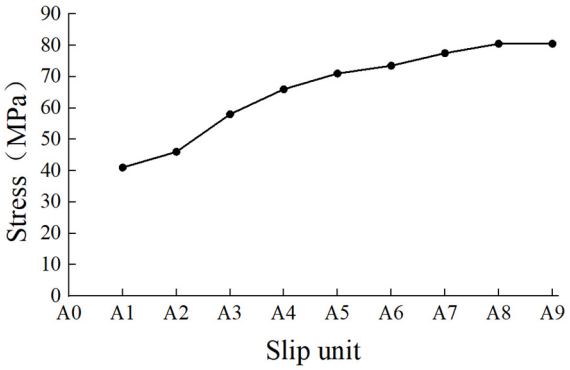


Figure 15. Stress change curve of the first unit control bar.

5.1.3. Tire Frame Checking

It can be seen from Figure 16 that the maximum horizontal displacement and the maximum vertical displacement of the inner ring slip-supported tire frame during construction were 36 mm and 7.2 mm, respectively, and the stress ratios were less than 0.9, which meet the construction requirements [29].

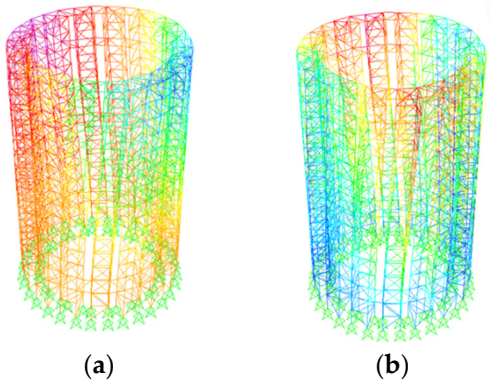
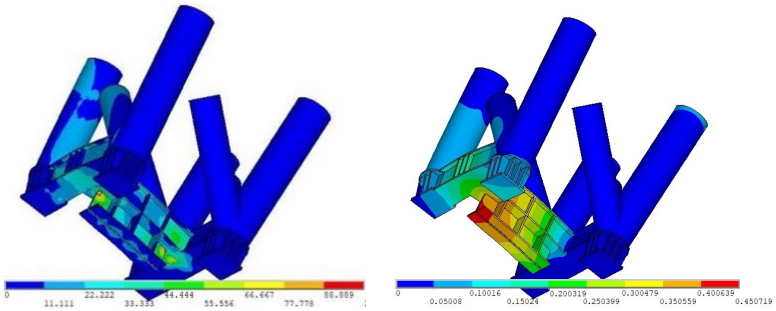


Figure 16. Deformation of an inner ring-supported tire frame (mm) (**a**) X-direction, (**b**) Z-direction.

5.1.4. Slipper Checking

The finite element software ANSYS was used to calculate the slipper; the unit type was set as Solid185; and the material was Q345B. According to the load transferred by the superstructure, the standard value for the maximum load bearing of the slipper bottom was 650 kN. Moreover, considering the dynamic effects, the design value of the vertical load was determined as 1.4 × 650 = 910 kN, with the analysis result shown in Figure 17.

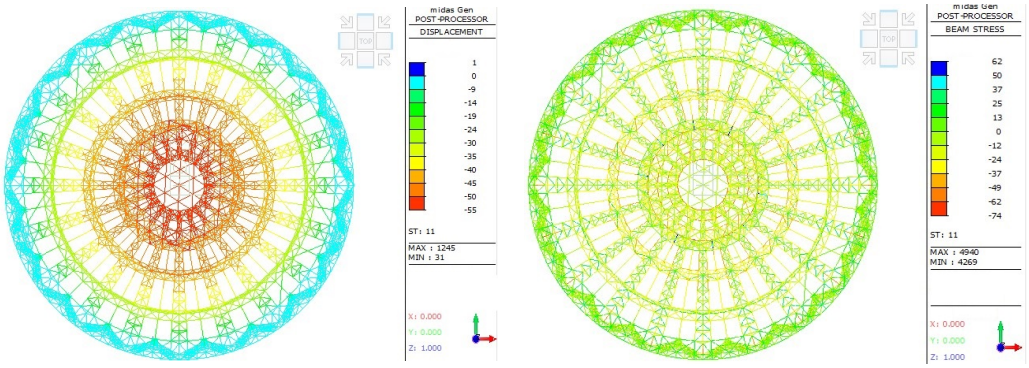


(**a**) (**b**)

Figure 17. Cloud diagram of slipper stress and deformation (mm). (**a**) Stress cloud diagram, (**b**) deformation cloud diagram.

5.2. Construction Process of Cable Structure

The cable structure's maximum tension stress and displacement occurred in the last stage. The displacement and stress of the steel structure after tension are shown in Figure 18; the cable structure stress is shown in Figure 19; the vertical displacement of each control node of the rod during the tensile process is shown in Figure 20.



(**a**) (**b**)

Figure 18. Displacement and stress cloud diagram of steel structure. (**a**) Displacement cloud diagram of steel structure after tension, (**b**) stress cloud diagram of steel structure after tension.

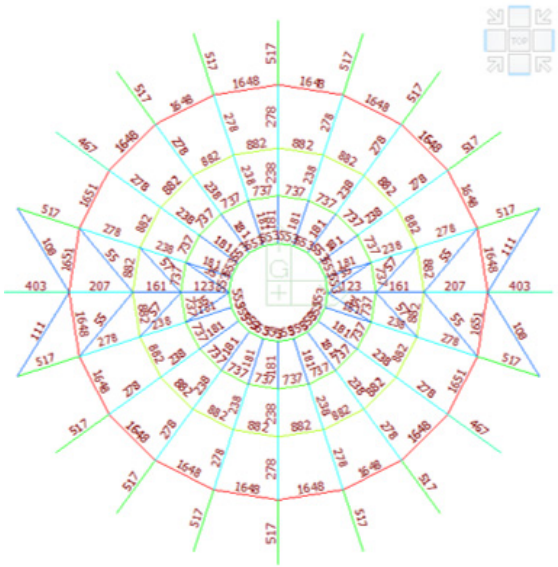


Figure 19. Tension cloud diagram of cable structure after tension.

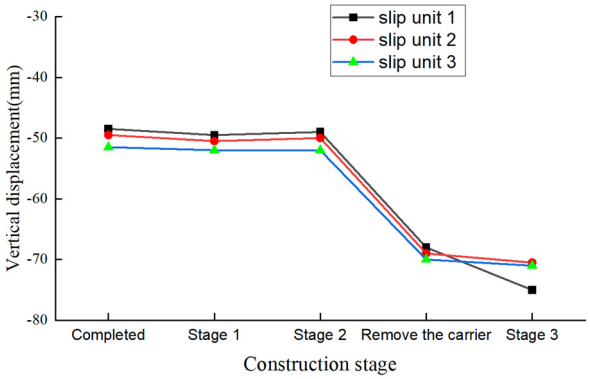


Figure 20. Vertical displacement of prestressed tensioning control nodes.

Figures 18 and 19 show that:

1. Before the completion of the first two tension stages without removing the central tire frame, the vertical deformation of the steel structure was small, with a maximum deformation of 20 mm. After removing the central tire frame and completing the third tension stage, the maximum deformation of the steel structure increased rapidly to 55 mm, but the deformation value was below the limit of the construction specifications. Hence, it meets the construction requirements;
2. During tension installation, the steel structure's maximum tensile and compressive stresses were 62 MPa and 74 MPa, respectively;
3. After removing the central tire frame and completing the third tension stage, the maximum tension of the annular cable was 1648 kN, and that of the radial cable was 517 kN;
4. After the completion of tension, the value of cable force gradually increased from inside to outside, and the cable force distribution was more uniform.

It can be seen in Figure 20 that:

1. In the first tension stage, the cables were tensioned in batches of up to 10% of the designed tension force, which slightly influenced the displacement and stress of the steel structure in the main gymnasium;
2. In the second tension stage, the cables were tensioned in batches of up to 70% of the designed tension, which could improve the vertical displacement of the roof truss of the main gymnasium by a minimum amplitude;
3. In the third tension stage, the cables were tensioned in batches to design tension. From the result, it can be seen that it had a very limited influence on structural displacement.

5.3. Auxiliary Gymnasium Construction Process

Since the steel structure in the auxiliary gymnasium was simpler than that in the main gymnasium, the truss part could be regarded as a three-span continuous beam, and the longest span was the middle one. The finite element software calculation shows that the midspan vertical displacement was very small, which is far from the degree required for safety. Moreover, the construction sequence of the tensioning cables in the main gymnasium was adopted after the auxiliary gymnasium installation. When tensioning the cables, the main structure had been installed and formed as a whole. Additionally, the structure was under reasonable stress. The installation of the auxiliary gymnasium and the tension of cables did not adversely affect the main gymnasium structure.

6. Comparison between Simulation and Monitoring Results

6.1. Comparative Analysis of Stress

Figure 21 compares the stress simulation (sim) and monitoring (mon) values of representative measuring points in the truss structure's upper chord, lower chord, and belly bar during the slip construction stage. It can be seen that although there were deviations be-

tween the simulation and monitoring results at some measuring points, the trends between the two were the same. There was a big difference between the simulation and monitoring results at the measuring points near the central ring because, for the simplified calculation, a supported tire frame for the central ring was set up in the model.

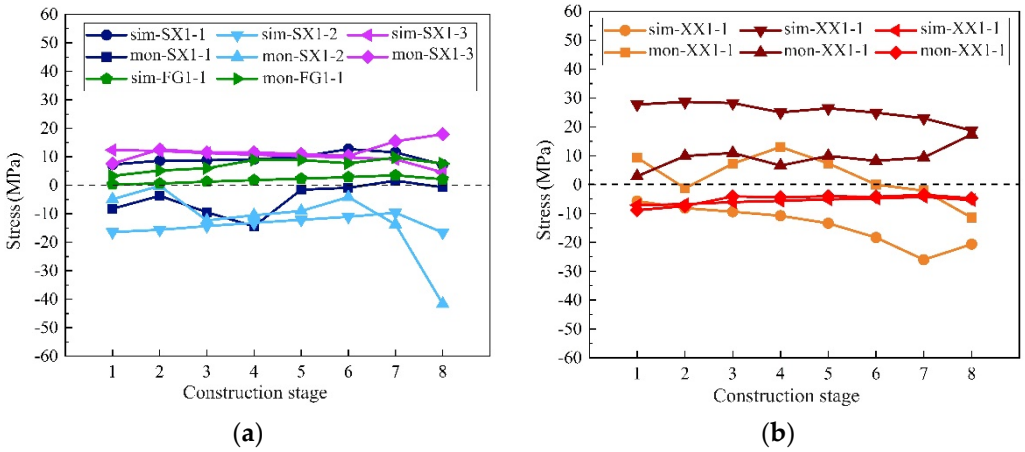


Figure 21. Comparison of stress results. (**a**) Measuring points on the upper chord and belly bar, (**b**) Measuring points on the lower chord.

6.2. Displacement Comparison Analysis

The bar displacement is an important control index in the space structure construction, and two measuring points on the lower chord of the radial inverted triangular truss were selected. The comparison of displacement results of each measuring point is shown in Figure 22. It shows that the structure's displacements along the X and Y directions were small during the construction process, and several measuring points underwent sudden changes during construction 5 and 6. Structural displacement mainly occurred in the Z (vertical) direction, but it presented a decreasing trend with the construction progress.

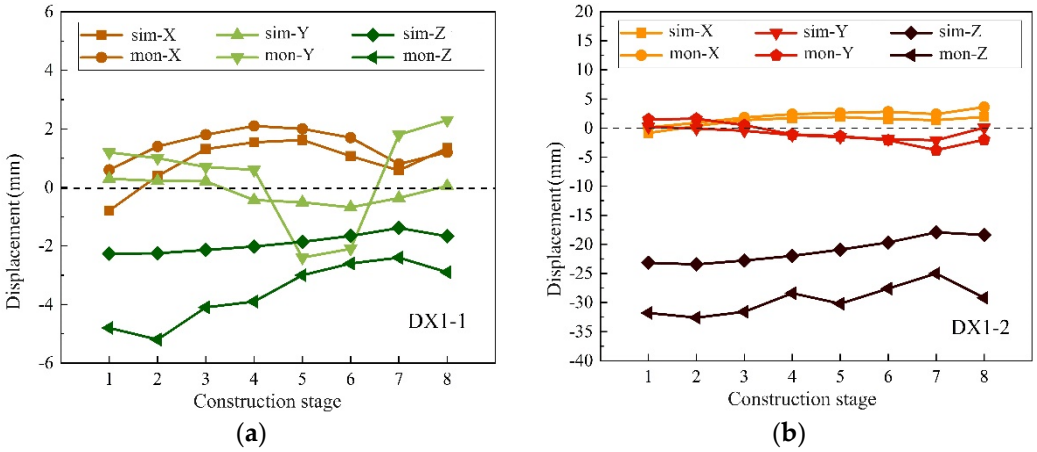


Figure 22. Comparison of displacement results. (**a**) DX1-1, (**b**) DX1-2.

Because a construction site is affected by many factors, such as temperature and weather, the structure is gradually stressed with sliding assembly, and the internal force displacement of bars is redistributed. This makes it difficult to achieve identical results with those of the simulation, which are calculated under ideal conditions. However, the changing trend of simulation and monitoring results were similar, and the joint displacement direction was the same, which indicates that the structure simulation calculation had certain accuracy and can provide the basis for formulating the structural monitoring scheme in construction.

7. Conclusions

This paper carries out the finite element simulation analysis and construction monitoring of a gymnasium's radial space truss suspended dome structure. The main conclusions are as follows:

1. The maximum deformation of the long-span space truss suspended dome structure increased from 23.89 mm to 25.40 mm and finally stabilized at 19.26 mm as the construction process gradually stabilized, and the internal force of the early bar was increasing. This indicates that the structural stiffness was gradually formed during the construction process, and the weak parts of the structure were changed compared to the one-time forming, meaning that it is necessary to analyze the construction process;
2. The finite element simulation results were relatively close to the measured data; the calculation result of stress and displacement was consistent with the variation trend of the simulation curve, and the stress characteristics of the bars were consistent with the displacement direction of the measuring point. The finite element numerical simulation can effectively reflect the structure's mechanical properties in the process of slip construction and provide a basis for the layout of monitoring points in the engineering site.
3. The displacement and internal force of the main gymnasium in the cumulative slip construction process met the code requirements, indicating that the construction scheme is reasonable and feasible, and can provide reference for similar engineering construction.
4. The tension of the prestressed cable had little effect on improving the roof's vertical displacement in the main gymnasium. Hence, it is necessary to fully consider the change of structural displacement and adjust it in a timely manner when unloading.
5. In view of the fact that the construction stage is only the initial state of the structure entering the service period, a long-term monitoring system for the use of the structure needs to be developed in order to investigate the continuous changes of the subsequent structural performance.

Author Contributions: Conceptualization, M.L. and J.Z.; methodology, Y.J.; software, C.H.; validation, C.Z. and C.H.; formal analysis, X.Y.; investigation, Y.Z.; resources, M.L.; data curation, Y.J.; writing—original draft preparation, Y.J.; writing—review and editing, C.H.; visualization, Y.J.; supervision, J.Z.; project administration, X.Y.; funding acquisition, M.L. All authors have read and agreed to the published version of the manuscript.

Funding: This study was funded by the Science and Technology Program of the Ministry of Housing and Urban-Rural Development (2020-K-126), the Research Project of Shaanxi Construction Group (2020-14-323), and the Training Plan for Young Key Teachers of the Institution of Higher Education in Henan Province (2019GGJS147).

Institutional Review Board Statement: Not applicable.

Informed Consent Statement: Not applicable.

Data Availability Statement: Data are contained within the article.

Conflicts of Interest: The authors declare that they have no known competing financial interests or personal relationships that could have appeared to influence the work reported in this paper.

References

1. Olofin, I.; Liu, R. Suspen-Dome System: A Fascinating Space Structure. *Open Civ. Eng. J.* **2017**, *11*, 131–142. [CrossRef]
2. Noshnagh, A.R. Suspen-Domes: Study of the Behaviour and the Design. University of Surrey: Guildford, UK, 2012.
3. Kang, W.; Chen, Z.; Lam, H.; Zuo, C. Analysis and design of the general and outmost-ring stiffened suspen-dome structures. *Engineering Struct.* **2003**, *25*, 1685–1695. [CrossRef]
4. Lin, L. Long-span Steel Structure System and Application Case Summary. *Highlights Sci. Eng. Technol.* **2022**, *18*, 155–161. [CrossRef]
5. Gong, S. The research of suspen-dome structure. *IOP Conf. Series Mater. Sci. Eng.* **2017**, *242*, 12050. [CrossRef]
6. Zhou, G. Key Construction Technology of Steel Structure in Dalian International Conference Center. *Prog. Steel Build. Struct.* **2012**, *14*, 53–58. (In Chinese)

7. Yousuf, D. Chronological Construction Sequence Effects on Reinforced Concrete and Steel Buildings. *Int. J. Eng. Sci.* **2014**, *3*, 52–63. [CrossRef]
8. Yao, G.; Wu, C.; Yang, Y. Scientometric Analysis for Mechanical Performance of Broken-Line Long-Span Steel Structure in Construction Considering Geometric Nonlinearity. *Symmetry* **2021**, *13*, 1229. [CrossRef]
9. Liu, R.; Li, M.; Cheng, T. Discussion on cable-strut systems of the suspen-dome structures. *Int. J. Space Struct.* **2022**, *8*, 15–22. [CrossRef]
10. Yan, R. Effect of Random Pre-stressed Friction Loss on the Performance of a Suspen-dome Structure. *Adv. Steel Constr.* **2022**, *7*, 27–32. [CrossRef]
11. Shen, Y.; Luo, Y. Accumulative Sliding Construction Method for Large-Span Latticed Shells. *J. Constr. Eng. Manag.* **2010**, *136*, 1154–1157. [CrossRef]
12. Ren, F.; Zhang, J.; Yuan, M.; Rao, D.; Yu, X.; Gao, Y.; Yu, D. Overhead Accumulative Sliding Construction Technology of Unequal Height of Large Span Spatial Steel. *IOP Conf. Series Mater. Sci. Eng.* **2018**, *392*, 022002. [CrossRef]
13. Zhou, Q.; Zhang, C.; Xiao, L.; Zhang, X.; Xie, Y. Study on the Influence of Excitation in Sliding Construction of Long Span Steel Structure. *IOP Conf. Series Earth Environ. Sci.* **2021**, *719*, 032010. [CrossRef]
14. Cui, C.; Sun, W.B. FEM Analysis of Long-Span Steel Structure Considering Bearings Size Effect and Friction Characteristic. *Appl. Mech. Mater.* **2013**, *351–352*, 812–817. [CrossRef]
15. Liu, H.; Han, Q.; Chen, Z.; Wang, X.; Yan, R.-Z.; Zhao, B. Precision Control Method for Pre-stressing Construction of Suspen-dome Structures. *Adv. Steel Constr.* **2014**, *10*, 404–425. [CrossRef]
16. Liu, H.; Chen, Z.; Zhou, T. Research on the Process of Pre-Stressing Construction of Suspen-dome Considering Temperature Effect. *Adv. Struct. Eng.* **2012**, *15*, 489–493. [CrossRef]
17. Fan, X.; Zhao, Z.; Xu, H.; Liu, H.; Zhang, N.; Wu, X. The Tensioning Process of Ellipsoidal Suspen-dome Structures with Considering the Friction of Cable-strut Joints. *Structures* **2021**, *34*, 3757–3775. [CrossRef]
18. Li, Z.; Zhang, Z.; Dong, S.; Fu, X. Construction Sequence Simulation of a Practical Suspen-dome in Jinan Olympic Center. *Adv. Steel Constr.* **2012**, *8*, 38–53. [CrossRef]
19. Du, W.; Zhu, L.; Sun, F. Improved Rigid Cable Method for Pre-Stress Optimization in Suspend-Dome Structures. *Appl. Mech. Mater.* **2013**, *438–439*, 815–818. [CrossRef]
20. Liu, J.; Meng, F.; Chen, Y.; Chen, Z. The influence of coupling on the whole process of construction simulation of chord dome structure. *E3S Web Conf.* **2020**, *143*, 01046. [CrossRef]
21. Liu, H.J.; Yang, L.F.; Li, Y.L.; Xu, H. Geometrically Nonlinear Analysis on a Double Controlled Form Finding Method Considering Construction Process of Suspen-Domes. *Adv. Mater. Res.* **2014**, *904*, 524–527. [CrossRef]
22. Zhou, Z.; Feng, Y.; Meng, S.; Wu, J. A novel form analysis method considering pretension process for suspen-dome structures. *KSCE J. Civ. Eng.* **2014**, *18*, 1411–1420. [CrossRef]
23. Liu, X.; Zhang, A.; Fu, W. Cable Tension Preslack Method Construction Simulation and Engineering Application for a Prestressed Suspended Dome. *Adv. Mater. Sci. Eng.* **2015**, *2015*, 651041. [CrossRef]
24. Teng, J.; Lu, W.; Cui, Y.; Zhang, R. Temperature and Displacement Monitoring to Steel Roof Construction of Shenzhen Bay Stadium. *Int. J. Struct. Stab. Dyn.* **2016**, *16*, 1640020. [CrossRef]
25. Pomares, J.C.; Pereiro-Barceló, J.; González, A.; Aguilar, R. Safety Issues in Buckling of Steel Structures by Improving Accuracy of Historical Methods. *Int. J. Environ. Res. Public Heal.* **2021**, *18*, 12253. [CrossRef]
26. Más, R.I.; Torres, J.C.; Reales, J.R. Prismatic structural members: Cross section flat and normal to the axis? *Rev. La Constr.* **2017**, *16*, 507–517. [CrossRef]
27. Xu, W.; Chen, D.; Qian, H.; Chen, W. Non-uniform Temperature Field and Effects of Large-span Spatial Truss Structure under Construction: Field Monitoring and Numerical Analysis. *Structures* **2021**, *29*, 416–426. [CrossRef]
28. Chen, D.S.; Xu, W.C.; Qian, H.L.; Sun, J.Y.; Li, J.F. Effects of Non-uniform Temperature on Closure Construction of Spatial Truss Structure. *J. Build. Eng.* **2020**, *32*, 101532. [CrossRef]
29. Ministry of Urban Rural Development of the People's Republic of China. *Technical Specification for Space Frame Structures: JGJ 7-2010[S]*; China Architecture & Building Press: Beijing, China, 2010; pp. 14–15. (In Chinese)
30. Liu, Y.; Chen, Z.; Zhang, Y. Construction Technique and Simulation Analysis of Large-span Spatial Steel Structure. *Int. Conf. Remote Sens. Environ. Transp. Eng.* **2011**, 1065–1068. [CrossRef]
31. Yang, W. Health monitoring and simulation analysis over construction loading process for long-span steel structure. *Spat. Struct.* **2012**, *18*, 49–54. (In Chinese)

Disclaimer/Publisher's Note: The statements, opinions and data contained in all publications are solely those of the individual author(s) and contributor(s) and not of MDPI and/or the editor(s). MDPI and/or the editor(s) disclaim responsibility for any injury to people or property resulting from any ideas, methods, instructions or products referred to in the content.